

Constraining the properties of the proposed supermassive black hole system in 3c66b: Limits from pulsar timing

Fredrick A. Jenet ¹, Andrea Lommen², Shane L. Larson³, Linqing Wen ³

ABSTRACT

Data from long term timing observations of the radio pulsar PSR B1855+09 have been searched for the signature of Gravitational waves (G-waves) emitted by the proposed supermassive binary black hole system in 3C66B. For the case of a circular orbit, the emitted G-waves would generate detectable fluctuations in the pulse arrival times of PSR B1855+09. General expressions for the expected timing residuals induced by G-wave emission from a slowly evolving, eccentric, binary black hole system are derived here for the first time. These waveforms are used in a Monte-Carlo analysis in order to place limits on the mass and eccentricity of the proposed black hole system. The reported analysis also demonstrates several interesting features of a gravitational wave detector based on pulsar timing.

Subject headings: pulsar:general - pulsar:individual (B1855+09) - gravitational waves - black hole physics

1. introduction

This letter reports on the search for Gravitational wave (G-wave) emission from the recently proposed Supermassive Binary Black Hole (SBBH) system in 3C66B (Sudou et al. 2003, S03 hereafter) using timing data from the radio pulsar PSR B1855+09. Given the length of the available data set (7 years) and this pulsar's low rms timing noise ($1.5 \mu\text{s}$), these data are well suited for this analysis. The proposed binary system has a current period of 1.05 years, a total mass of $5.4 \times 10^{10} M_{\odot}$, and a mass ratio of 0.1. Given the close proximity

¹California Institute of Technology, Jet Propulsion Laboratory
4800 Oak Grove Drive, Pasadena, CA 91109

²Franklin and Marshall College, Department of Physics and Astronomy, PO Box 3003, Lancaster, PA 17604

³California Institute of Technology, 1500 California Blvd. , Pasadena CA, 91125

of the radio galaxy 3C66B ($z = 0.02$), the G-waves emitted by this system could induce a detectable signature in the timing residuals of PSR B1855+09, with a maximum residual amplitude of order $10 \mu\text{s}$, assuming the eccentricity of the system is zero and the Hubble constant is 75 km/s/Mpc .

The analysis of these data will demonstrate two interesting properties of a gravitational wave detector made up of radio pulsars. First, the amplitude of the observed signature increases with decreasing gravitational wave frequency. Second, the light travel time delay between the Earth and the pulsar can, depending on the geometry, allow one to observe the gravitational wave source at two distinct epochs of time simultaneously. For example, if the pulsar is 4000 light-years away and the Earth-pulsar line-of-sight is perpendicular to the G-wave propagation vector, then the observed timing residuals will contain information about the source both at the current epoch and 4000 years ago. If the G-wave emitter is a binary system, slowly inspiraling due to G-wave emission, then the observed residuals will contain both low and high frequency components. The difference in the frequencies of these components will depend on how quickly the system is evolving. Since pulsar timing is more sensitive to lower frequencies, the highest amplitude oscillations in the timing residuals will be due to the delayed (i.e. 4000 year old) component. This effect, referred to as the “two-frequency response”, is analogous to the 3-pulse response occurring in spacecraft doppler tracking experiments (Estabrook & Wahlquist 1975) and the multi-pulse response from time-delay interferometry used in the proposed Laser Interferometer Space Antenna (LISA) mission (Armstrong, Estabrook, & Tinto 1999).

The next section describes the expected signature of G-wave emission from a general binary system and for the specific case of the proposed system in 3C66B. The observations of PSR B1855+09 used to search for G-waves are described in section 3. Section 4 discusses the search techniques employed as well as the Monte-Carlo simulation used to place limits on the mass and eccentricity of the system, and the results are discussed in section 5.

2. The Signature of 3C66B

The orbital motion of the proposed binary system in 3C66B will generate gravitational radiation. The emitted G-waves will induce periodic oscillations in the arrival times of individual pulses from radio pulsars. Given a model for the pulse arrival times in the absence of G-waves, one can generate a time series of “residuals” which are the observed pulse arrival times minus the expected pulse arrival times. Ideally, the effects of known accelerations are removed from the timing residuals leaving only the variations due to the presence of G-waves.

The emitted G-waves are described by two functions of spacetime, $h_+(t)$ and $h_\times(t)$ which correspond to the gravitational wave strain of the two polarization modes of the radiation field. As these waves pass between the Earth and a pulsar, the observed timing residuals, $R(t)$, will vary as (Estabrook & Wahlquist 1975; Detweiler 1979)

$$R(t) = \frac{1}{2}(1 + \cos(\mu))(r_+(t) \cos(2\psi) + r_\times(t) \sin(2\psi)), \quad (1)$$

where μ is the angle between the pulsar line-of-sight and the G-wave source, ψ is the G-wave polarization angle and the “+” and “ \times ” refer to the two G-wave polarization states. The functions r_+ and r_\times , referred to collectively as $r_{+,\times}$, are related to the gravitational wave strain by

$$r_{+,\times}(t) = r_{+,\times}^e(t) - r_{+,\times}^p(t) \quad (2)$$

$$r_{+,\times}^e(t) = \int_0^t h_{+,\times}^e(\tau) d\tau \quad (3)$$

$$r_{+,\times}^p(t) = \int_0^t h_{+,\times}^p(\tau - \frac{d}{c}(1 - \cos(\mu))) d\tau, \quad (4)$$

where $h_{+,\times}^e(t)$ is the gravitational wave strain at Earth, $h_{+,\times}^p(t)$ is the gravitational wave strain at the pulsar, t is time, τ is the time integration variable, d is the distance between Earth and the pulsar, and c is the speed of light. Note that the pulsar term, $h_{+,\times}^p$, is evaluated at the current time minus a geometric delay which encodes the time it takes the G-waves to propagate from the source to the pulsar plus the time it takes the pulses from that instant to propagate from the pulsar to Earth. Hence, $r_{+,\times}^e$ is induced by waves emitted at a later epoch than those that induce $r_{+,\times}^p$.

G-waves emitted by a system in a circular orbit (i.e. zero eccentricity) will vary sinusoidally as a function of time with a frequency given by twice the orbital frequency. For eccentric systems, the emitted waves will contain several harmonics of the orbital frequency. The 2nd harmonic will dominate at low eccentricities while the fundamental (i.e. the orbital) frequency will dominate at high eccentricities. In general, the period and eccentricity of a binary system will be decreasing with time due to the fact that the system is radiating away energy and angular momentum in G-waves. Hence, the frequencies present in $h_{+,\times}(t)$ will vary with time. Since $r_{+,\times}^e$ and $r_{+,\times}^p$ may be generated by $h_{+,\times}(t)$ at epochs separated by an extremely long time interval, the frequency content of these terms may differ significantly.

The G-wave strain, $h(t)$, induced by a black hole binary may be calculated using the standard weak field approximation applied to two orbiting point masses (Wahlquist 1987). The expected residuals are found by integrating $h(t)$ with respect to time (see Eqs. 2 - 4):

$$r_+^e(t) = \alpha(t)(A(t) \cos(2\phi) - B(t) \sin(2\phi)) \quad (5)$$

$$r_{\times}^e(t) = \alpha(t)(A(t)\sin(2\phi) + B(t)\cos(2\phi)), \quad (6)$$

$$\alpha(t) = \frac{M_c^{\frac{5}{3}}}{D\omega^{\frac{1}{3}}} \frac{\sqrt{1 - e(t)^2}}{1 + e(t)\cos(\theta(t))} \quad (7)$$

where D is the distance to the source, ϕ is the orientation of the line of nodes on the sky, $\omega(t)$ is the orbital frequency, $e(t)$ is the eccentricity, $\theta(t)$ is the orbital phase, and M_c is the “chirp mass” defined as

$$M_c = M_t \left(\frac{m_1 m_2}{M_t^2} \right)^{\frac{3}{5}} \quad (8)$$

where $M_t = m_1 + m_2$ and m_1 and m_2 are the masses of the individual black holes. Note that all units from Equation 5 on are in “geometrized” units where $G = c = 1$ ⁴. $A(t)$ and $B(t)$ are given by

$$\begin{aligned} A(t) &= 2e(t)\sin[\theta(t)]\{\cos[\theta(t) - \theta_n]^2 - \cos[i]^2\sin[\theta(t) - \theta_n]^2\} - \\ &\quad \frac{1}{2}\sin[2(\theta(t) - \theta_n)]\{1 + e(t)\cos[\theta(t)]\}\{3 + \cos[2i]\} \end{aligned} \quad (9)$$

$$B(t) = 2\cos[i]\{\cos[2(\theta(t) - \theta_n)] + e(t)\cos[\theta(t) - 2\theta_n]\} \quad (10)$$

where i and θ_n are the orbital inclination angle and the value of θ at the line of nodes, respectively (Wahlquist 1987). $\theta(t)$ and $e(t)$ are given by the following coupled differential equations (Wahlquist 1987; Peters 1964):

$$\frac{d\theta}{dt} = \omega(t) \frac{\{1 + e(t)\cos[\theta(t)]\}^2}{\{1 - e(t)^2\}^{\frac{3}{2}}} \quad (11)$$

$$\frac{de}{dt} = -\frac{304}{15} M_c^{\frac{5}{3}} \omega_0^{\frac{8}{3}} \chi_0 \frac{e(t)^{-\frac{29}{19}} [1 - e(t)^2]^{\frac{3}{2}}}{[1 + \frac{121}{304}e(t)^2]^{\frac{1181}{2299}}}, \quad (12)$$

where ω_0 is the initial value of $\omega(t)$ and χ_0 is a constant that depends on the initial eccentricity e_0 :

$$\chi_0 = [1 - e_0^2][e_0^{-\frac{12}{19}}][1 + \frac{121}{304}e_0^2]^{\frac{-870}{2299}}. \quad (13)$$

$\omega(t)$ is given by

$$\omega(t) = a_0 e(t)^{-\frac{18}{19}} [1 - e(t)^2]^{\frac{3}{2}} [1 + \frac{121}{304}e(t)^2]^{-\frac{1305}{2299}}, \quad (14)$$

where a_0 is determined by the initial condition $\omega(t = 0) = \omega_0$. The above equations are accurate to first order in v/c , and valid only when both $e(t)$ and $\omega(t)$ vary slowly with time. The expressions for $r_{+, \times}^p$ are identical to those for $r_{+, \times}^e$. Note that $r_{+, \times}^p$ is evaluated at an earlier time than $r_{+, \times}^e$ (See Eqs. 3 and 4).

⁴In geometrized units, mass and distance are in units of time.

For the specific case of the S03 parameters for 3C66B, the high chirp mass ($1.3 \times 10^{10} M_{\odot}$) together with the period of 1.05 years implies a lifetime of ≈ 5 years. The orbital period of such a system will be evolving rapidly. The angle between 3C66B and PSR B1855+09 on the sky is 81.5° and PSR B1855+09 lies 1 ± 0.3 kpc away (Kaspi, Taylor, & Ryba 1994, hereafter KTR94). The total time delay between the pulsar epoch and the Earth epoch is given by $(d/c)(1 - \cos(\mu))$ which is equal to 3700 ± 1100 years (see Eq. 4) for these objects. Since the time delay between the Earth and the pulsar is much larger than the timescale for evolution of the system, the expected residual will contain a low frequency component due to the pulsar term ($r_{+,x}^p$) and a high frequency component due to the Earth term ($r_{+,x}^e$). The top panel in Figure 1 shows a theoretical set of timing residuals due to G-wave emission from the proposed binary system in 3C66B assuming that the distance to this galaxy is 80 Mpc and the distance to the pulsar is 1 kpc. This waveform was generated with $i = \theta_n = \phi = 0$ and $\psi = \pi/4$. The chirp mass used was $1.3 \times 10^{10} M_{\odot}$ and the orbital period at the epoch of the S03 observations (i.e. MJD= 51981) was taken to be 1.05 years. The eccentricity at this epoch was taken to be .0001. Two distinct oscillation frequencies can be seen, one with a period of about .88 years and the other with a period around 6.24 years. The bottom panel in Figure 1 shows the Lomb periodogram of the simulated residuals. The Lomb periodogram is the analogue of the discrete Fourier transform for unevenly sampled data and is further discussed in §4. The simulated residuals demonstrate two important features of an Earth-pulsar gravitational wave detector. The first is that it is more sensitive to low frequency oscillations. The second is that a single set of timing residuals can contain information about the source from two widely separated epochs of time. The low frequency seen here was due to the orbital period 3700 years ago.

3. Timing Observations of PSR B1855+09

We used observations of PSR B1855+09 made by Kaspi, Taylor, & Ryba (1994) (hereafter KTR94) at the Arecibo Observatory 300 m telescope ¹ and made public therein. The KTR94 data set is made up of more than 7 years (1986-1993) of bi-weekly observations using the Princeton University MarkIV system. The data were corrected for small errors in the observatory UTC clock as compared to GPS time, for errors in GPS time as compared to UTC as maintained by the National Institute of Standards and Technology and finally for errors in UTC(NIST) as compared to terrestrial time (TT) as maintained by the Bureau International des Poids et Mesures (Guinot 1988). For more details on data acquisition,

¹The National Astronomy and Ionosphere Center Arecibo Observatory is operated by Cornell University under contract with the National Science Foundation

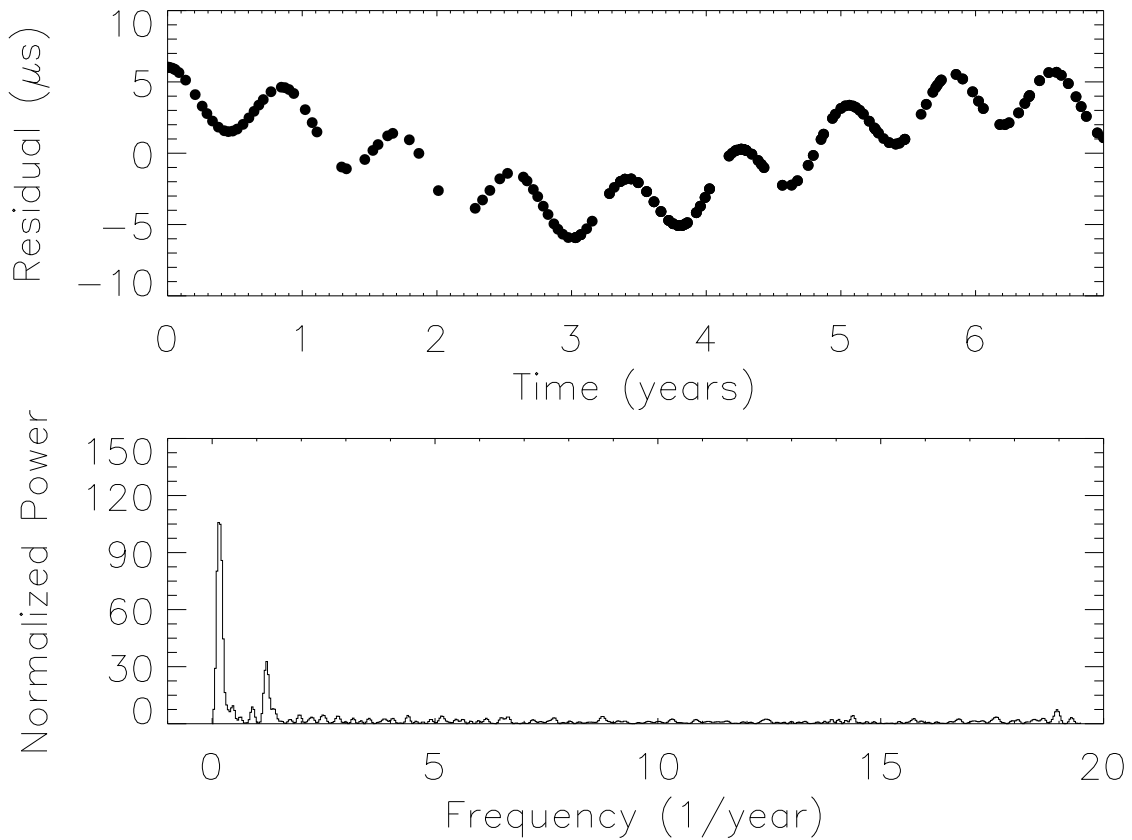


Fig. 1.— Top panel: Theoretical timing residuals induced by G-waves from 3C66B. The timing points are chosen to coincide with the actual timing residuals of B1855+09. Bottom panel: The corresponding normalized Lomb periodogram.

reduction, and clock correction, please see KTR94.

Using the standard TEMPO software package ⁵ the TOAs were fit to the model published by KTR94. We used their best-fit values as our initial parameters. In the fitting we allowed the spin period (P), period derivative (\dot{P}), right ascension, declination, proper motion, parallax, and the 5 Keplerian binary parameters to vary. Additionally, the Shapiro delay parameters were included in the model but were fixed at the optimum values published by KTR94. The best-fit values of all parameters were consistent with those published by KTR94. The resulting timing residuals used are shown in the top panel of Figure 2.

4. Constraints from pulsar timing

The timing residuals from PSR B1855+09 were searched for the signature of G-waves using the normalized Lomb periodogram (see Press, Teukolsky, Vetterling, & Flannery (1992) section 13.8) together with “harmonic summing.” The Lomb periodogram (LP) is the analog of the discrete Fourier transform for unevenly sampled data. Harmonic summing is performed by adding together the periodogram power at harmonics of each frequency up to a chosen maximum harmonic (Lyne 1988). This process increases the sensitivity to periodic, non-sinusoidal waveforms like those expected from eccentric binaries. If a SBBH system existed in 3C66B with an eccentricity of zero and a chirp mass and period adopted by S03, then the LP should show the two-frequency response like that seen in Figure 1. Figure 2 plots the normalized LP for the residual data described above. The periodogram power was calculated for 542 frequencies ranging from $1/27.8 \text{ year}^{-1}$ to 19.5 year^{-1} with a resolution of $1/27.8 \text{ year}^{-1}$. This corresponds to a frequency oversampling factor of 4. There are no significant peaks in this LP. For purposes of this paper, a significant peak has less than a .1% chance of occurring in purely random data assuming Gaussian statistics. Harmonic summing was performed up to the 6th harmonic. Again, no significant features were found.

Since the LP analysis was unable to detect the presence of G-waves in the timing residuals, limits can be placed on the possible chirp mass and eccentricity of the system. Since the general waveform given by Eqs. 5-7 depends on various unknown quantities that specify the orientation of the orbit and the viewing geometry, a Monte-Carlo simulation was performed in order to determine the probability of detecting a SBBH system in 3C66B with a given chirp mass and eccentricity. Aside from M_c and e , the general wave form depends on 6 angles: two angles specify the plane of the orbit, two determine the orbital phase of binary at the beginning of each of the two relevant epochs, and two determine the initial location

⁵<http://pulsar.princeton.edu/tempo>

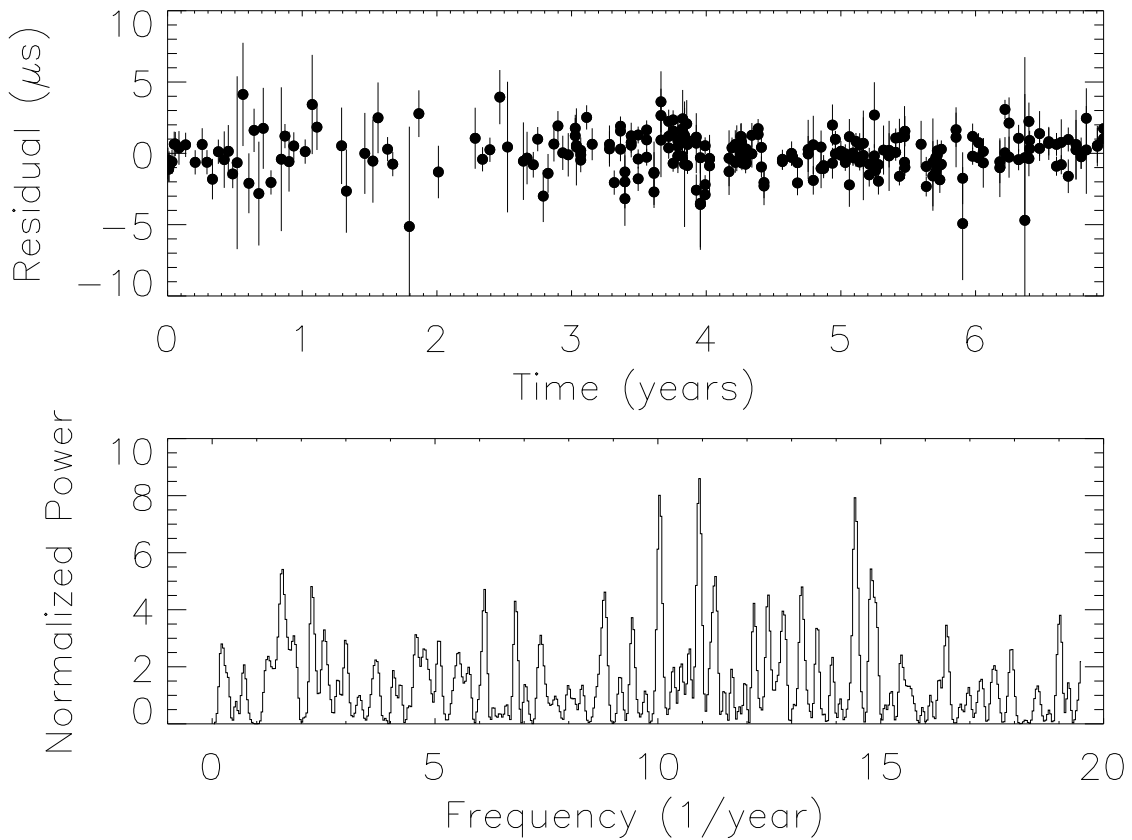


Fig. 2.— Top Panel: Timing residuals for B1855+09. Bottom Panel: The corresponding normalized Lomb periodogram.

of the line of nodes at the start of each epoch. For a given M_c and e , the initial eccentricities and periods were determined using Eqs. 11 and 12. An orbital period of 1.05 years at MJD = 51981 was chosen for the initial parameters in order to match the observations of S03. The distances to 3C66B and B1855+09 were taken to be 80 Mpc and 1 kpc, respectively. The 6 unknown angles were chosen at random from a uniform distribution that ranged from 0 to 2π and a corresponding waveform was generated using Eqs. 5-14. The waveform was then added to the residual data. When processing the timing data, the program TEMPO will remove the effects of the Earth’s orbit and parallax together with a linear trend. In order to simulate the effects of removing these components from the data, various functions were subtracted from the simulated data. A 1 year periodicity was removed by subtracting a function of the form $y = a \cos(\omega t) + b \sin(\omega t)$ where t is time, $\omega = 2\pi/1$ year, and a and b were determined by a least-squares fit to the simulated data. A 6 month periodicity was removed in a similar fashion. A best fit first order polynomial was also removed. This combination of data plus simulated signal minus various fitted functions was then analyzed using the Lomb periodogram method described above. If a significant peak was found (see above), then the signal was considered to be detected. 1000 waveforms were tested for each M_c and initial e . It was found that there is a 98% chance of detecting a system like that adopted by S03 if it has an eccentricity less than 0.03. As the eccentricity increases above 0.03, the system is evolving rapidly enough to make the period at the earlier epoch (i.e. the period in the pulsar term), much longer than the observation length. Hence, for eccentricities between 0.03 and 0.49, the probability drops to about 95%. The detection probability starts falling off again above eccentricities of 0.49. At this point, the period of binary system at the start of the observations is longer than the observing time. The results for this and other chirp masses are summarized in table 1. The first column lists the chirp mass in $10^{10}M_\odot$, the next four columns list the limiting eccentricities at the 98%, 95%, and 90% probability levels. For example, with $M_c = 1.0$, if the eccentricity at the epoch of the S03 observations was less than 0.03, then there was at least a 95% chance of detecting the system in these data using the techniques described above.

5. Conclusions

The signature of G-waves emitted by the proposed system in 3C66B was not found in the analysis of the pulsar timing residuals of PSR B1855+09. The system adopted by S03 has a total mass of $5.4 \times 10^{10}M_\odot$ and a chirp mass of $1.3 \times 10^{10}M_\odot$. The confidence with which such a system can be ruled out depends on its eccentricity, which is not constrained by the S03 observations. It is generally accepted that the eccentricity of a system near coalescence will be small, but exactly how small depends on many unknown aspects of the

system’s formation and evolution. If the eccentricity is less than 0.03, then the adopted system may be ruled out at the 98% confidence level. As the assumed eccentricity of the system increases, its expected lifetime will decrease. Given that the system had to exist for longer than one year, it can be shown that the eccentricity must be less than 0.3 for a black hole binary system with negligible spins (Bardeen, Press, & Teukolsky 1972). In this case, the system can be ruled out at the 95% confidence level.

Even though the adopted system is highly unlikely, it is possible that the system has a lower chirp mass. A system with a chirp mass less than $0.7 \times 10^{10} M_{\odot}$ cannot be ruled out from the timing data regardless of the eccentricity. Systems with chirp masses of $1.0 \times 10^{10} M_{\odot}$ and $0.8 \times 10^{10} M_{\odot}$ become more and more allowable when the eccentricities are larger than 0.18 and 0.03, respectively.

The above discussion assumed a value of 75 km/s/Mpc for the Hubble constant. For other values, the chirp masses listed in Table 1 need to be multiplied by a factor of $(H/75)^{-3/5}$ where H is the desired Hubble constant in units of km/s/Mpc. Since the actual Hubble constant is expected to lie within the range of 65 to 85 km/s/Mpc, the chirp masses listed in Table 1 are valid to within 10%.

Aside from a lower mass binary black hole system, there are other possible explanations for the S03 observations. The most obvious is that the observed precession is a systematic effect arising from the Earth’s orbit. On the other hand, if the observed precession is real, then the observed position angles of the two ellipses may be explained by wandering of the emission region along the jet as various shocks propagate within the jet (see for example Marscher et al 1991).

This analysis demonstrates how pulsar timing measurements may be used to search for G-waves from SBBH systems. In the future, pulsar timing will become more sensitive to SBBH systems as radio astronomers learn how to reduce the observed noise in pulsar timing data and/or more stable radio sources are discovered. The residual waveforms presented here will be useful in searching such high quality data for the signatures of SBBH systems. The two-frequency response may also provide an interesting tool for studying the physics of such systems since it will provide information about the SBBH system at two distinct epochs of time.

Part of this research was performed at the Jet Propulsion Laboratory, California Institute of Technology, under contract with the National Aeronautics and Space Administration. AL acknowledges support of NSF grant #0107342. The authors wish to thank John Armstrong for useful discussions.

REFERENCES

Armstrong, J. A., Estabrook, F. B. & Tinto, M. 1999, *ApJ*, 527, 814

Bardeen, J. M., Press, W. H., & Teukolsky, S. A. 1972, *ApJ*, 178, 347

Detweiler, S. 1979, *ApJ*, 234, 1100

Estabrook, F. B. & Wahlquist, H. D. 1975, *General Relativity and Gravitation*, 6, 439

Guinot, B. 1988, *A&A*, 192, 370

Kaspi, V. M., Taylor, J. H., & Ryba, M. F. 1994, *ApJ*, 428, 713

Lyne, A. G. in *Gravitational Wave Data Analysis* (NATO ASI Series), ed. Schutz D. (Reidel, Dordrecht), p. 95

Marscher, A. P., Zhang, Y. F., Shaffer, D. B., Aller, H. D., & Aller, M. F. 1991, *ApJ*, 371, 491

Peters, P. C., *Phys. Rev.*, 136, 1224

Press, W. H., Teukolsky, S. A., Vetterling, W. T., & Flannery, B. P. 1992,

Sudou, H., Iguchi, S., Murata, Y., & Taniguchi, Y. 2003, *Science*, 300, 1263

Wahlquist, H. 1987, *General Relativity and Gravitation*, 19, 1101

Table 1. Detection Limits

M_c ($10^{10} M_\odot$)	98%	95%	90%	M_c ($10^{10} M_\odot$)	98%	95%	90%
1.3	0.03	0.49	0.51	1.0	—	0.03	0.18
1.2	0.02	0.49	0.51	0.9	—	0.02	0.04
1.1	0.02	0.16	0.23	0.8	—	0.01	0.03
				0.7	—	—	—

Note. — Given a chirp mass, M_c , and a minimum detection probability, this table lists the maximum eccentricity the proposed system can have at the epoch of the S03 observations. A “—” means that the probability of detecting the system never reached the specified value.